




## DYNAMIC SIMULATION AND MODELING OF A NOVEL COMBINED HYBRID PHOTOVOLTAIC-THERMAL PANEL HYBRID SYSTEM

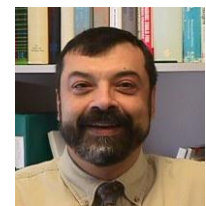
 S. Sami<sup>1\*</sup>

 C. Campoverde<sup>2</sup>

<sup>1</sup>Research Center for renewable Energy Catholic University of Cuenca, Cuenca, Ecuador, USA

<sup>1</sup>Email: [dr.ssami@transpacenergy.com](mailto:dr.ssami@transpacenergy.com) Tel: 619 272 9131

<sup>2</sup>TransPacific Energy, Inc, NV, USA



(+ Corresponding author)

### ABSTRACT

#### Article History

Received: 26 December 2017

Revised: 23 January 2018

Accepted: 26 January 2018

Published: 1 February 2018

#### Keywords

Dynamic modeling

Simulation

Photovoltaic-thermal solar hybrid

system

Numerical

Model validation.

A novel combined concept and simulation model of a hybrid photovoltaic-thermal solar panel hybrid system are presented. This concept is developed to enhance the energy conversion efficiency of the PV cell and utilize excess thermal energy dissipated by the conversion process to produce domestic hot water. A heat transfer and fluid flow two dimensional dynamic model was developed to describe the behavior of a combined photovoltaic cell-thermal panel hybrid system under different solar irradiance, material properties, and boundary conditions. The model is based on dynamic mass and energy equations coupled with the heat transfer coefficients, and thermodynamic constants as well as material properties.

**Contribution/Originality:** This paper presents a significant contribution into the development of a novel hybrid system of solar photovoltaic-thermal solar that can significantly enhance the energy conversion efficiency of the solar photovoltaic solar panels, produce electricity as well as hot water for domestic or industrial applications.

### 1. INTRODUCTION

Global warming and other environmental factors are influencing decisions by organizations in the energy industry to develop green new energy technologies for both commercial and residential markets. The PV cell technology was invented in 1894 by Charles Fritts, where sunlight is converted into electrical energy. This energy can be harnessed and supplied to the electrical grid or used in remote areas. However, currently, the efficiency of commercial solar PV is to up to 15% and more than 35% of incoming solar radiation energy is either absorbed or reflected (Lalovi *et al.*, 1986; Bergene and Lovvik, 1995; Teo *et al.*, 2012; Yang *et al.*, 2012) and therefore, significant excess heat is lost. New PV technologies reported in the literature (Lalovi *et al.*, 1986; Huang and Du, 1991; Bergene and Lovvik, 1995; Garge and Agarwal, 1995; Sandnes and Rekstad, 2002; Chen *et al.*, 2011; Teo *et al.*, 2012; Yang *et al.*, 2012; Gangadevi *et al.*, 2013) have been shown to improve energy utilization efficiency of solar PV, such as multi-junction cells, optical frequency shifting, and concentrated photovoltaic (CPV) systems, among others; however, are expensive.

In order to improve the solar PV's efficiency a novel concept of combined photovoltaic-thermal solar panel hybrid system concept has been developed (Huang and Du, 1991; Bergene and Lovvik, 1995; Garge and Agarwal, 1995; Sandnes and Rekstad, 2002; Chen *et al.*, 2011; Teo *et al.*, 2012; Gangadevi *et al.*, 2013). It is simple hybrid system where the PV cells are cooled through water flows. The solar irradiance is converted into electrical energy in the PV's cell; however, excess thermal energy is generated and dissipated due to the intrinsic conversion efficiency limitation of the cell. The dissipated and excess thermal energy increases the cell temperature and in turn reduces the conversion efficiency of the cell. The excess thermal energy absorbed by the cold water flow through the heat exchanger thermal panel underneath the PV's cell can be used for various domestic or industrial applications. Therefore, the net result is an enhancement of the combined photovoltaic-thermal efficiency of the hybrid system.

The conceptual design for a photovoltaic thermal (PV/T) solar panel has been developed and analyzed, to control the inherent temperature increase of PV cells to increase electrical efficiency (Lalovi *et al.*, 1986; Huang and Du, 1991; Bergene and Lovvik, 1995; Garge and Agarwal, 1995; Sandnes and Rekstad, 2002; Chen *et al.*, 2011; Teo *et al.*, 2012; Yang *et al.*, 2012; Gangadevi *et al.*, 2013). A hybrid solar panel has been developed and presented by Yang *et al.* (2012) to integrate photovoltaic (PV) cells onto a substrate through a functionally graded material (FGM) with water tubes cast inside, through which water serves as both heat sink and solar heat collector. Yang *et al.* employed a heat transfer two dimensional model to describe a steady state system of a combined photovoltaic cell-thermal panel system (Bergene and Lovvik, 1995) with suitable values of solar irradiance, material properties, and boundary conditions were used as initial parameter values for the modeling. Another novel hybrid solar power generation system (HSPGS) was proposed by (Li *et al.*, 2010; Li, 2015). It mainly consists of photovoltaic/thermal (PV/T) collectors based on amorphous silicon (a-Si) cells, Organic Rankine Cycle (ORC), and inner-type heat storage unit. The PV/T collectors produce electricity directly via the cells, and the waste heat is carried away to the ORC for thermal power generation. Zhan *et al.* (2014) proposed a 20kW design capacity solar parabolic dish concentrator hybrid solar/gas dish Stirling system (HS/GDSS). To ensure a steady operation of an electricity power plant, HS/GDSS uses gas as complement when solar radiation is weak. Thermodynamic models were developed and presented to conduct design of system parameters.

A novel combined concept and simulation model of photovoltaic-thermal solar panel hybrid system are presented in this study. This novel concept is intended to enhance the energy conversion efficiency of the PV-Thermal solar hybrid system through using utilizing excess thermal energy dissipated by the conversion process to produce domestic hot water. The conceptual photovoltaic-thermal panel design was modeled and analyzed using a two dimensional dynamic model based upon the heat transfer and fluid flow conversion equations. The model was developed to describe the steady state and dynamic behavior of a combined photovoltaic cell-thermal panel hybrid system under solar irradiance, material properties, ambient and fluid flow conditions and excess thermal energy recovered by the panel as well as boundary conditions. The predicted results presented herein include the efficiency of energy conversion of the hybrid system, PV cell and the amount of excess thermal energy recovered by the panel and transferred to the heat exchanger fluid flow under different conditions. A schematic of the thermal solar system under study is depicted in Figure.1.

## 2. MATHEMATICAL MODEL

The study presented herein is based on the work previously reported by Yang *et al.* (2012) and Gangadevi *et al.* (2013); Chen *et al.* (2011) where a flat plate solar collector is attached to a PV panel. The hybrid system is composed of the PV solar panel and Thermal solar tube collector (Tripanagnostopoulos *et al.*, 2002). The PV solar panel-and-tube, water cooled PVT was analyzed in this work. It consists of a photovoltaic panel welded on the backside and thin parallel tubes for the circulation of the cooling fluid. The various flow tubes in contact with the PV solar panel are connected to a thermal tank from which water flows through the solar collector copper pipes and carry the excess heat away from the PV and thermal panel as shown in Figure 1. As this study investigates forced convection

using water as the coolant, and as the heat transferred fluid HTF, various water flow rates at different conditions will also be analyzed to assess their impact on cooling performance of the PV system.

On the other hand, Figure.2 describes the PV basic diagram, where the PV panels output in DC current are connected to the load controller and batteries as well as the inverter for converting the DC current output into AC current for potential use in applications where AC is required.

The end result is power generation by the PV solar panels with the thermal excess heat is transferred to produce domestic hot water DHW. The enhancement in the hybrid system efficiency of the solar PV panel at various operating temperatures will be calculated by the model presented in the following sections.

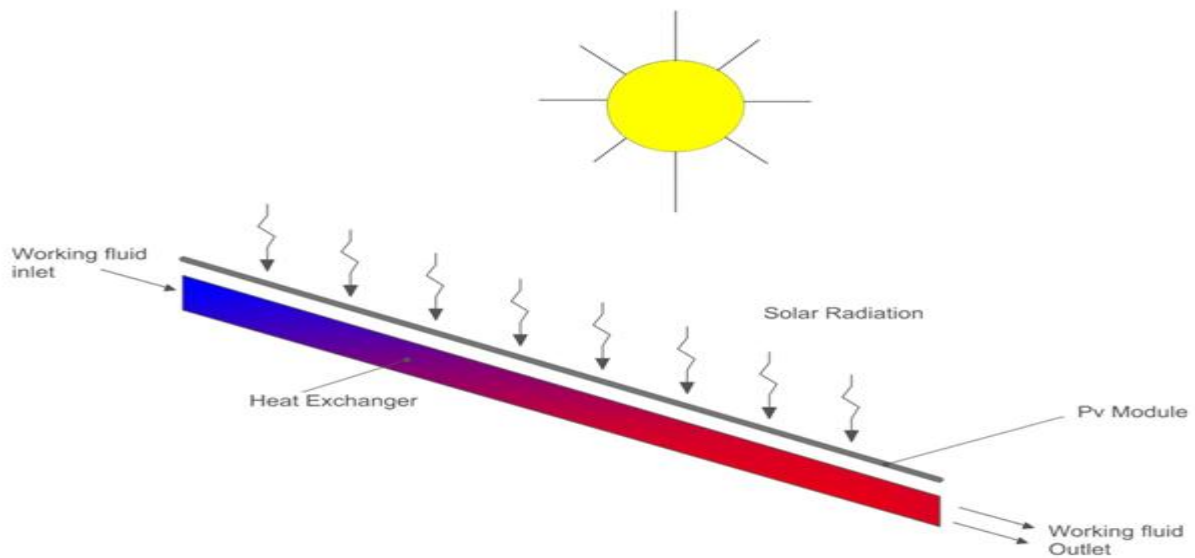


Figure-1. PV/Thermal hybrid system

### 3. PV THERMAL MODEL

The following thermal analysis is performed for the PV cell, however, it is assumed that all PV cells behave the same; therefore, it is applied to the PV solar panel.

The heat absorbed by the PV solar cell can be calculated by the following (Zhan *et al.*, 2014; Sami and Marin, 2017; Sami and Rivera, 2017)

$$Q_{in} = \alpha_{abs} G S_p \tag{1}$$

Where;

$\alpha_{abs}$ : Overall absorption coefficient

G : Total Solar radiation incident on the PV module

$S_p$ : Total area of the PV module

Meanwhile, the PV cell Temperature is computed from the following heat balance (Fargali *et al.*, 2010; Sami and Marin, 2017; Sami and Marin, 2017; Sami and Rivera, 2017)

$$mC_{p\_module} \frac{dT_C}{dt} = Q_{in} - Q_{conv} - Q_{elect} \tag{2}$$

Where;

$T_C$ : Pv Cell Temperature

$mC_{p\_module}$ : Thermal capacity of the PV module

t: time

$Q_{in}$ : Energy received due to solar irradiation

$Q_{conv}$ : Energy loss due to Convection

$Q_{elect}$ : Electrical power generated

And the Solar energy absorbed by the PV cell,  $Q_{in}$ , is given by equation (1).

The energy loss due to heat convection can be obtained from;

$$Q_{conv} = S_p H(T_C - T_a) \quad (3)$$

H: Convective heat transfer coefficient

$T_a$ : Ambient temperature

The electrical power generated is given by;

$$Q_{elect} = \eta G S_c \quad (4)$$

$\eta$ : Module efficiency

$S_c$ : Total surface area of PV cells in a module

### 3.1. Thermal Energy Incident in a PV Cell

The thermal energy transferred from the PV cell to the Heat Transfer Fluid (HTF) is determined from the heat balance across the PV cell and the heat transfer mechanisms of the HTF, in terms of the conduction, convection and radiation;

The heat transfer by conduction is;

$$Q_{conduction} = \frac{Q_{in\_cell}}{Area_{cell}} \quad (5)$$

$Area_{cell}$ : PV cell area

$Q_{in\_cell}$ : Energy incident on a PV cell due to solar radiation

$Q_{conduction}$ : Energy due to conduction

Equation (5) can be rewritten as;

$$Q_{conduction} = \frac{K_{Pv} \times \Delta T(T_c - T_m)}{L_{cell}} \quad (6)$$

$T_m$ : Module Back-surface temperature

$K_{Pv}$ : Thermal conductivity of PV cell

$L_{cell}$ : Length of a PV cell

The heat transfer by convection is determined from;

$$Q_{convection} = h_{water} \times \Delta T(T_m - T_f) \quad (7)$$

$Q_{convection}$ : Energy due to convection

$h_{water}$ :heat tranfer coefficient

$T_f$ :Fluid temperature

And the heat transfer by radiation is;

$$Q_{radiation} = \varepsilon \times \sigma(T_m^4 - T_f^4) \quad (8)$$

$Q_{convection}$ : Energy due to radiation

$\varepsilon$ : Emissivity of the PV cell

$\sigma$ : Stefan-Boltzmann constant

The heat transfer fluid flow rate, water, is determined from the following equations (9) through (11);

$$m_{water} = \frac{\rho \times L_{cell} \times \frac{\pi \times D^2}{4}}{nTE} \quad (9)$$

Where;

$m_{water}$ : mass of water

$\rho$ : density of liquid water

D: Internal Pipe diameter

nTE: number of Thermal Elements in a pipe

And,

$$\frac{\partial Q}{m_{water} C_p} = \frac{Q_{convection} \times Area_{pipe}}{m_{water} \times C_{p\_water} \times nTE} \quad (10)$$

Area<sub>pipe</sub>: Pipe area

$\partial Q$ : Convection heat transfer rate

$C_{p\_water}$ : Thermal capacity of water (4186 J/kgK)

And,

$$Q_{convection} = \dot{m} \times C_{p\_water} \times T_{fHx} / Area_{pipe} \quad (11)$$

$\dot{m}$ : Water flow

$T_{fHx}$ : Maximum temperature difference at the Heat Exchanger heat tubes.

The finite-difference formulation is used to determine the heat transfer fluid temperature that follows at each element of the heat transfer fluid and it worthwhile noting that the heat transfer fluid tube is divided into,  $nTE$ , elements;

$$T_f = T_{f\_in} + \frac{\partial Q}{m_{water} C_p} \times t \quad (12)$$

Where,

t: time

$T_{f\_in}$ : Fluid temperature at inlet

The thermal energy transferred from the PV cell to the heat transfer fluid is obtained by;

$$Q_{Thermal} = \dot{m} \times C_{p\_water} \times \Delta T (T_{fHx+1} - T_{f\_in}) \quad (13)$$

$Q_{Thermal}$ : Energy from thermal process

$T_{fHx+1}$ : Fluid temperature at thermal element (1)

The energy transferred to heat transfer fluid is calculated by the integration of equations (12) and (13) written for each element,  $dx$ , along the length of each tube.

The PV cell and solar panel temperature is influenced by different factors and in particular the ambient conditions such as the temperature, humidity, wind speed among other parameters. In order to evaluate the impact of the humidity on the air temperature, the following equation is considered. Based on the Ideal Gas Law the humidity ratio can be expressed as <https://en.wikipedia.org/wiki/Humidity>:

$$x = \frac{0.62198 p_w}{(p_a - p_w)} \quad (14)$$

And;

$x$  : humidity ratio (kg water/kg dry air)

$P_w$  : partial pressure of water vapor in moist air (Pa)

$P_a$  : atmospheric pressure of moist air (Pa)

Where the ambient dry temperature and  $P_w$  are interrelated by the following relationship,

[http://www.engineeringtoolbox.com/water-vapor-saturation-pressure-air-d\\_689.html](http://www.engineeringtoolbox.com/water-vapor-saturation-pressure-air-d_689.html)

$$p_w = \frac{\rho_w T_{db}}{0.022} \quad (15)$$

Where;

$\rho_w$ : Density of water vapor

$T_{db}$ : Dry bulb temperature

The back temperature  $T_m$  of the PV cell and PV panel can be calculated from the heat balance across the PV cell as follows [http://www.engineeringtoolbox.com/water-vapor-saturation-pressure-air-d\\_689.html](http://www.engineeringtoolbox.com/water-vapor-saturation-pressure-air-d_689.html)

$$Q_{in} = m C_{p\_module} \Delta T = m C_{p\_module} (T_C - T_m) \quad (16)$$

Where;  $T_m$  is the module back-surface temperature.

It is assumed that the  $T_m$  is equal to the surface temperature of the heat exchanger tubes welded to the solar PV cell/panel in close contact to the back surface of each of the PV cells. The heat transferred from the back of the PV cell to the heat transfer fluid HTF flowing in the heat exchanger tubes is computed by the following forced heat transfer convection relationship (Duffie, 1991; Fargali *et al.*, 2010).

$$Q_{in} = \pi D L h_{water} \Delta T = \pi D L h_{water} (T_m - T_f) \quad (17)$$

Where;

D: Pipe diameter

L: Pipe length

$h_{water}$ : Forced convection heat transfer coefficient

$T_f$ : Fluid temperature

The heat transfer fouling factor was estimated under the following conditions; cooling water less than 50 °C, and cooling fluid greater than 120 °C and water velocity under 1m/s using the following [http://www.engineeringtoolbox.com/fouling-heat-transfer-d\\_1661.html](http://www.engineeringtoolbox.com/fouling-heat-transfer-d_1661.html).

$$h_d = \frac{1}{\left(R_d + \frac{1}{U}\right)} \quad (18)$$

Where,

$h_d$  : Thermal conductance of heat exchanger after fouling (W/m<sup>2</sup>K)

$U$  : Thermal conductance of clean heat exchanger (W/m<sup>2</sup>K)

$R_d$  : The fouling factor - or unit thermal resistance of the deposit, City grid/Treated Boiler Feed water; 0.00018 m<sup>2</sup>K/W, where the heat transfer coefficient,  $h_d$ , is approximated as Sami and Rivera (2017);

$$h = \frac{K_w}{D_H} b_2 Re^n \quad (19-a)$$

$$Re = \frac{m_w D_H}{\mu A_f} \quad (19-b)$$

Where Re; is the Reynolds number.

In this analysis, the main stream temperature of the heat transfer fluid flow is considered as the average temperature of the inlet and outlet of the each finite difference element;

$$T_f = \frac{T_{inlet} + T_{outlet}}{2} \quad (20)$$

Where;

$T_{inlet}$  : Water temperature inlet at each element.

$T_{outlet}$  : Water temperature outlet at the end of a pipe element

To calculate the heat transfer fluid flow rate in the pipe, equation (21) is used as follows;

$$Q_{in} = \dot{m}_w m C_{p\_water} (\Delta T)$$

And;

$$Q_{in} = \dot{m}_w C_{p\_water} (T_{f+1} - T_f) \quad (21)$$

$\dot{m}_w$  : Water flow.

$T_{f+1}$  : Water temperature at the next element.

$C_p$ : Specific heat of HTF.

Where,  $\dot{m}$  is defined as;

$$\dot{m}_w = \frac{\pi D^2}{4} v \rho_{water} \quad (22)$$

Where,

$v$  : Fluid velocity

$\rho_{water}$  : Water density

### 3.2. PV Model

The solar photovoltaic panel is constructed of various modules and each module is consisted of arrays and cells. The dynamic current output can be obtained as follows (Fargali *et al.*, 2010; Sami and Marin, 2017; Sami and Marin, 2017; Sami and Rivera, 2017).

$$I_p = I_L - I_o \left[ \exp \left( \frac{q(V + I_p R_s)}{AkT_c} - \frac{V + I_p R_s}{R_{sh}} \right) \right] \quad (23)$$

$I_p$ : Output current of the Pv module

$I_L$  : Light generated current per module

$I_o$  : Reverse saturation current per module

$V$  : Terminal voltage per module

$R_s$  : Diode series resistance per module

$R_{sh}$  : Diode shunt resistance per module

$q$ : Electric charge

$k$  : The Boltzman constant

$A$  : Diode ideality factor for the module

Where; reverse saturation current per module can be obtained as follows,

$$I_o = BT^3 c \left[ \exp \left( -\frac{E_{go}}{KT_c} \right) \right] \quad (24)$$

And; light generated current per module is;

$$I_L = P_1 G [1 - P_2 (G - G_r) + P_3 (T_c - T_r)] \quad (25)$$

Where;

The PV cell temperature,  $T_c$ , is influenced by various factors such as solar radiation, ambient conditions, and wind speed. It is well known that the cell temperature impacts the PV output current, performance and its time-variation can be determined from references (Sandnes and Rekstad, 2002; Fargali *et al.*, 2010; Li *et al.*, 2010; Gangadevi *et al.*, 2013; Zhan *et al.*, 2014; Li, 2015; Sami and Marin, 2017; Sami and Marin, 2017; Sami and Rivera, 2017).

### Battery Charging and Discharging Model

The battery stores excess power is controlled by the load charge controller (C.F Figure.2). The battery keeps voltage within the specified voltage and thus, protects over discharge rates, and prevent overload.

During the charging period, the voltage-current relationship can be described as follows (Sandnes and Rekstad, 2002; Fargali *et al.*, 2010; Li *et al.*, 2010; Gangadevi *et al.*, 2013; Zhan *et al.*, 2014; Li, 2015; Sami and Marin, 2017; Sami and Rivera, 2017).

$$V = V_r + \frac{I \left( \frac{0.189}{(1.242 - SOC) + R_i} \right)}{AH} + (SOC - 0.9) \ln \left( 300 \frac{I}{AH} + 1.0 \right) \quad (26)$$

And;

$$V_r(V) = 2.094 [1.0 - 0.001(T - 25^\circ C)] \quad (27)$$

However, during the discharging process and using equation (23), the current-voltage can be;



$$V = V_r + \frac{I}{AH} \left( \frac{0.189}{soc} + R_i \right) \quad (28)$$

And  $R_i$  is given by;

$$R_i(\Omega) = 0.15[1.0 - 0.02(T - 25^\circ C)] \quad (29)$$

Where,

$V_r(V)$ , and  $I$ : the terminal voltage and current respectively

$R_i(\Omega)$ : Internal resistance of the cell and  $T$  is the ambient temperature.

$AH$ : Ampere-hour rating of the battery during discharging process

Finally, the power produced by the PV array can be calculated by the following equation,

$$P = V I_p \quad (30)$$

Where  $I_p$  is given by equation (23).

### Charge Controller

Generally, the controller power output (CF Figure.2), is given by (Sandnes and Rekstad, 2002; Fargali *et al.*, 2010; Li *et al.*, 2010; Gangadevi *et al.*, 2013; Zhan *et al.*, 2014; Li, 2015; Sami and Marin, 2017; Sami and Marin, 2017; Sami and Rivera, 2017).

$$P_{Cont-dc} = V_{bat}(I_{rct} + I_{PV} + I_{orc}) \quad (31)$$

Where;  $V_{bat}$  is multiplication of the nominal voltage DC in the battery for any particular system and  $I_{rct}$ ,

$I_{PV}$  and  $I_{orc}$  represent the output current of the rectifier in DC and currents of PV ./

### Inverter:

The characteristics of the inverter (CF Figure.2), are given by the ratio of the input power to the inverter  $P_{inv-ip}$  and inverter output power  $P_{inv-op}$ . The inverter will incur conversion losses and to account for the inverter efficiency losses,  $\eta_{inv}$  is used (Sandnes and Rekstad, 2002; Fargali *et al.*, 2010)

$$P_{inv-ip} \cdot \eta_{inv} = P_{inv-op} \quad (32)$$

The AC power of the inverter output  $P(t)$  is calculated using the inverter efficiency  $\eta_{inv}$ , output voltage between phases, neutral  $V_{fn}$ , and for single-phase current  $I_o$  and  $\cos\phi$  as follows;

$$P(t) = \sqrt{3} \eta_{inv} V_{fn} I_o \cos\phi \tag{33}$$

Finally, the hybrid system energy conversion efficiency for harnessing energy from solar PV and solar thermal is given by;

$$\eta_{hs} = \frac{P(t) + Q_{th}}{Q_{in}} \tag{34}$$

Where  $Q_{th}$  and  $Q_{in}$  are the solar thermal heat transferred to the HTF and solar irradiance. The respective values are given by equations (1) and (22), respectively. In addition,  $P(t)$  is the PV solar electrical output and defined by equation (33).

### Numerical Procedure

The energy conversion and heat transfer mechanisms taking place during various processes PV-Thermal shown in Figures.1 and 2, are described in Equations (1) through (34). The model presented hereby is based on mass and energy balances of the individual components of the PV/T hybrid system; PV cell and the heat transfer fluid flowing in thermal tubes welded in the back of the PV panel. This permits to calculate the electrical power output of the PV panel and characteristics of the water flow in terms of solar radiation and other geometry parameters. The aforementioned equations have been solved as per the logical flow diagram presented in Figures 3, where, the input parameters of the solar PV conditions such as solar radiation, ambient temperature and humidity as well as other independent parameters are defined. Dependent parameters were calculated and integrated in the system of finite-difference formulations. Iterations were performed until a converged solution is reached with acceptable iteration error. The numerical procedure starts with using the solar radiation, ambient conditions to calculate the solar PV cell temperature, and PV cell back temperature as well as heat transfer fluid mass flow rate circulating in the thermal closed loop at specified conditions. The thermodynamic and thermo physical properties of Heat Transfer Fluid were employed to calculate the water flow rate. This follows by using the finite-difference formulations to predict the time variation of the PV cell temperature, the PV back temperature, and thermal heat transferred to the Heat Transfer Fluid (HTF), outlet temperature of the heat transfer fluid at the heat exchanger, as well as other hybrid system power outputs and efficiencies. Finally, hybrid system efficiency is calculated at each input condition.

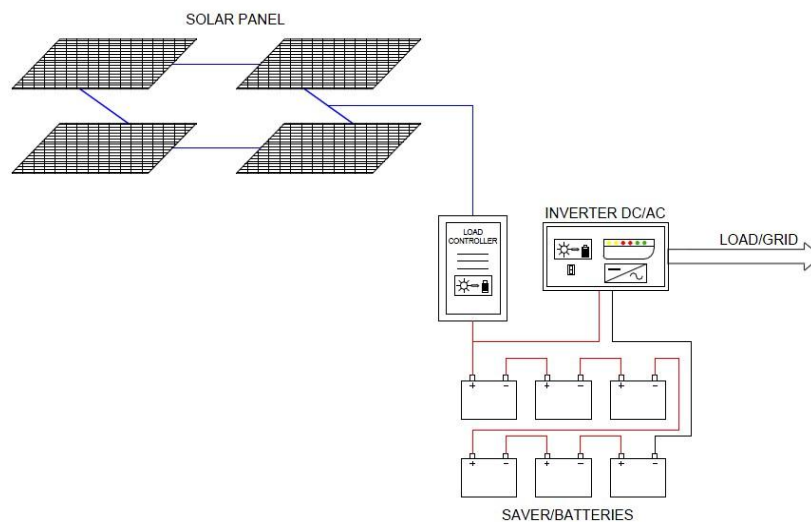


Figure-2. Proposed hybrid system; PV system

#### 4. RESULTS AND DISCUSSION

In order to solve the aforementioned equations (1) through (34) and taking into account the heat and mass transfer during the PV solar thermal conversion process, as discussed, the above mentioned equations were coded with finite-difference formulations and solved as per logical flow chart depicted in Figure.3. In addition, for the purpose of validation, the predicted simulated results for PV solar panel were compared to the data published in the literature under various conditions.

In the following sections, we present analysis and discussions of the numerical results predicted as well as validations of the proposed simulation model. The simulations were performed for temperature difference across the heat exchanger flow pipe of 5, 10, 15, 20 and 25 °C. However, only results will be presented and analyzed for the temperature difference of 15 °C across the thermal tube. It is worthwhile noting that the numerical simulation presented hereby was conducted under different conditions such as; PV cell temperatures from 10°C through 38°C, ambient temperatures from 10°C through 38°C and solar radiations; 550, 750, 1000 and 1200 w/m<sup>2</sup>.

Figures 4 and 5 present a typical ambient temperature and solar isolation profiles at the site for various months of the year 2015 and 2016 at different hours of the day. It is quite apparent that the peak solar irradiation and maximum temperatures occur at midday. However, average solar irradiation and ambient temperatures were used in the modeling and simulation of the Photovoltaic panels. The recording of the ambient conditions during this period showed that the relative humidity is stable during the various hours of the day. Therefore, in the simulation of the PV thermal solar panel relative humidities were assumed constant.

The PV characteristic curves are given in the manufacturer's specification sheet. The PV panel under consideration in this study are obtained from Fargali *et al.* (2010). Among the parameters used in this study are; Total surface area of the PV module (SP) is 0.617 m<sup>2</sup>, Total surface area of cells in module (Sc) is 0.5625 m<sup>2</sup>, module efficiency 12% at reference temperature (298 K), overall absorption coefficient is 0.73, and Temperature coefficient is 0.0045 K<sup>-1</sup>. Interested readers in the full range values of the other parameters are advised to consult (Fargali *et al.*, 2010).

It is also assumed in this simulation that the whole panel is covered in PV cells, with no packing material (material used to fill in gaps between the cells on a panel. The PV cells are commercial grade monocrystalline silicon cells with electrical efficiency of 12%, and have a thermal coefficient, of 0.54% [1/K] (Fargali *et al.*, 2010). The thermal coefficient represents the degradation of PV cell output per degree of temperature increase. The cooling heat exchanger pipes are bonded to the back of the PV solar model without any air gap to ensure complete heat transfer by conduction, convection and radiation to the fluid flowing in the thermal pipe.

As per equations (6) through (22), an increase in the PV cell temperature will result in an increase in the back cell temperature and consequently the fluid temperature due to the heat transfer by from solar energy by conduction and convection as well as radiation, respectively. Furthermore, Figures 6 through 8 demonstrate aforementioned statement that the higher the cell temperature the higher the back cell and fluid temperatures.

The effects of the PV panel operating temperature on the output efficiency have been well documented in the literature (Armstrong and Hurley, 2010; Bradley and Ernesto, 2012) where increasing temperature of the PV cell decreases the amount of power available. In order to evaluate the efficiency of a PV system, the temporal temperature variations are often regarded as instantaneous in steady state models. However, it is important to note that the changes in the PV cell temperature caused by solar radiation have a dynamic nature. The PV panel heats up and cools down gradually depending upon the changes in solar radiation in a dynamic response and consequently the power output from the PV panel.

In order to study and analyze the dynamic behavior of the PV cell temperature, back cell temperature as well as the fluid temperature, figures 6 through 8 have been plotted at different solar radiations, constant ambient temperature as well as heat exchanger temperature difference of 15 °C. It is quite evident from the results presented in these figures that the cell temperatures as well as the other ones increase with the increase of solar radiation.

This can be interpreted as per equations (1) and (2), where the higher the solar radiations the higher the energy absorbed by the PV cell and consequently the higher the temperature of the cell until reaches the design temperature.

The dynamic behavior of the thermal energy absorbed by the fluid flow flowing beneath the PV solar cell is determined by equations (17) and (18) and plotted in Figure 9 under different solar radiations. The results presented in these figure show that the higher the solar radiations the higher the thermal energy absorbed. The figure also shows that once the cell temperature stabilizes the thermal energy absorbed reaches the steady state level. On the other hand, the results also indicated that the systems stabilized after 1200 second and the desired water flow outlet was reached after this time elapse as shown in Figure.10.

Furthermore, the variation of the mass flow rate of the fluid flow at different time steps is also presented in Figure.10 at various solar radiations. As expected the fluid mass flow rate increased at higher solar radiation. This is due to the fact that the higher solar radiation results in higher thermal energy transferred to the fluid flow at constant temperature difference across the fluid flow thermal pipe and consequently this increases the fluid flow mass flow rate. Furthermore, the results presented in this figure also suggest that the fluid flow mass flow rate is quasi constant during the thermal conversion process.

The convective thermal energy converted and transferred to the fluid flow flowing under beneath the PV cell is depicted in Figure.11, where the energy conversion efficiency is plotted at different solar radiation at different time steps. The thermal efficiency is defined as the heat transferred divided by the solar radiation absorbed by the PV panel. It is quite evident from the results presented in this figure that the higher the solar radiation the higher the thermal conversion efficiency. On the other hand, the figure also shows that at higher time span the thermal energy conversion efficiency diminishes.

The hybrid system temperatures at difference interfaces were plotted and presented in Figure.12 at different solar radiations and heat exchanger temperature difference 15 °C. It is quite clear the higher the solar radiations the higher the interfacial temperatures. The temperature gradient presented in this figure shows that the heat flow from the solar energy is converted to the thermal heat energy that is absorbed by the heat transfer fluid, and clearly illustrated the impact on the different temperatures of the PV cell, the PV back temperature and the fluid temperature.

Furthermore, Figure. 13 displays the hybrid system efficiency at different solar radiations and heat exchanger temperature difference 15 °C. This efficiency is defined by equation (34). It appears from the results presented in this figure that the hybrid system efficiency is slightly reduced at higher solar radiation. This is attributed to the fact at higher solar radiation more heat losses are encountered during the heat flow process.

Furthermore, the different individual efficiencies of the hybrid system are presented in Figure .14 and compared to the hybrid system efficiency for heat exchanger temperature difference 15 °C. The performance of the hybrid PVT in terms of thermal efficiency, PV efficiency, electric PV efficiency and hybrid system efficiency is plotted in this figure as function of the solar radiations. It should be noted that the thermal efficiency is defined by the amount of thermal energy absorbed by the fluid flow divided by the solar radiation. On the other hand, the PV efficiency is the ratio between the output of the PV solar panel and the solar energy as defined by equation (30). The electric PV efficiency is the electric output calculated by equation (33) divided by the solar radiation. The climatic parameters; such as solar radiation, ambient temperature, humidity and wind speed were used to calculate the efficiencies presented in this figure. It is quite evident from this the results presented in this figure that using the thermal heat recovered from the solar radiation emitted from the PV solar panel to heat up the water flow enhances significantly the energy conversion efficiency of the PV system and the hybrid system efficiency. However, the efficiency of the PV Thermal remains roughly constant around the value of 24% since the temperature of the panel does not vary significantly due to the heat dissipated and absorbed by the heat transfer fluid.

The temperature difference between the PV cell temperature and the fluid temperature which is the thermal potential driver for heat flow from the PV cell to the fluid is plotted against the hybrid system efficiency at different solar radiations in Figure. 15. The results presented in this figure clearly show that the higher the solar radiation the higher the temperature difference and the higher hybrid system efficiency. In particular, it can be observed that at constant solar radiation, the results show that higher efficiency occurs at higher temperature difference. This is attributed to the fact that higher temperature difference between the PV cell temperature and the fluid flow, results in increase in heat flow from the solar energy to the fluid that causes that effect. Furthermore, Figure. 16 has been constructed to show the impact of the PV cell temperature on the power generated by the PV cell. It is quite evident from the results displayed in that figure that the power increases with increase of the cell temperature. Furthermore, this increase is limited by the maximum temperature allowed by the PV semiconductor material and design. This observation has been in agreement with others in the literature as long as the increase in the PV cell temperature was within the limitation imposed by manufacturer.

As mentioned previously the fluid temperature difference across the heat transfer tube was varied between 5 through 25 °C. Figure. 17 presents the thermal tubes heat transfer fluid flow rate at different temperature difference at different solar radiations. As expected the higher the solar radiation the higher the fluid mass flow rate. This observation has been explained elaborated in the aforementioned sections. On the other hand, it can be seen from the results presented in this figure that as the temperature difference across the heat transfer tubes increases mass flow rate decreases which is expected from the heat balance across the heat transfer tube as discussed previously.

Figures 18 and 19 were constructed to demonstrate the effect of varying the temperature difference across the heat transfer tube on thermal recovery efficiency and hybrid efficiency at different solar radiations. It is evident from the results presented in this figure as expected that the higher the solar radiations the higher the thermal and hybrid efficiencies. It should also be noted that the hybrid efficiency exhibits lower values than the thermal efficiency since the PV solar panel efficiency is significantly lower than the thermal efficiency.

#### 4.1. Model Validation

In order to validate our numerical model prediction described in equations (23) through (33), we have constructed Figures. 20 and .21 to compare the proposed model predicted numerical results with data presented in the literature for solar PV namely references (Fargali *et al.*, 2010; Sami and Rivera, 2017). In particular, it is quite apparent from the comparison presented in Figure. 20 that the model prediction fairly compares with the data of the dynamic PV cell temperature presented by Fargali *et al.* (2010). The comparison presented in this figure also showed that the model and data have the same trend, however, some discrepancies exit. It is believed that the discrepancies are due to the fact that the Fargali *et al.* (2010) did not provide full disclosure of the various parameters used in equations (23) through (33) and Reference (Rajapakse and Chungpaibulpantana, 1994) had to be consulted on the various missing parameters in Fargali *et al.* (2010). However, as pointed out in references (Rajapakse and Chungpaibulpantana, 1994; Sami and Rivera, 2017) taking into account the complexity of the PV cell temperature phenomena and its thermal behavior, we feel that our model fairly predicted the PV cell dynamic profile.

## 5. CONCLUSIONS

The energy conversion equations describing the mass and energy balances have been developed, integrated, coded and solved to predict the dynamic total power generated, efficiencies and other key important parameters of a hybrid system composed of a novel combined concept of a photovoltaic-thermal solar panel hybrid system. The predicted results have been presented under different solar irradiance, material properties, and boundary conditions. The model is based on dynamic mass and energy equations coupled with the heat transfer coefficients, and thermodynamic constants and as well as material properties.

It is evident from the results presented that the higher the solar radiations the higher the thermal and hybrid efficiencies. It is also observed that the hybrid efficiency exhibits lower values than the thermal efficiency since the PV solar panel efficiency is significantly lower than the thermal efficiency.

Furthermore, the PV simulation study results showed that the higher the solar radiation the accelerated increase in the PV cell temperature. Consequently, it also shows the higher the solar radiation the higher the PV power and PV amperage. It is imperative that the designer of the PV panel and its cell temperature should take into consideration the solar radiation as well as the ambient conditions. Finally, the model prediction compared fairly with the PV data at different conditions.

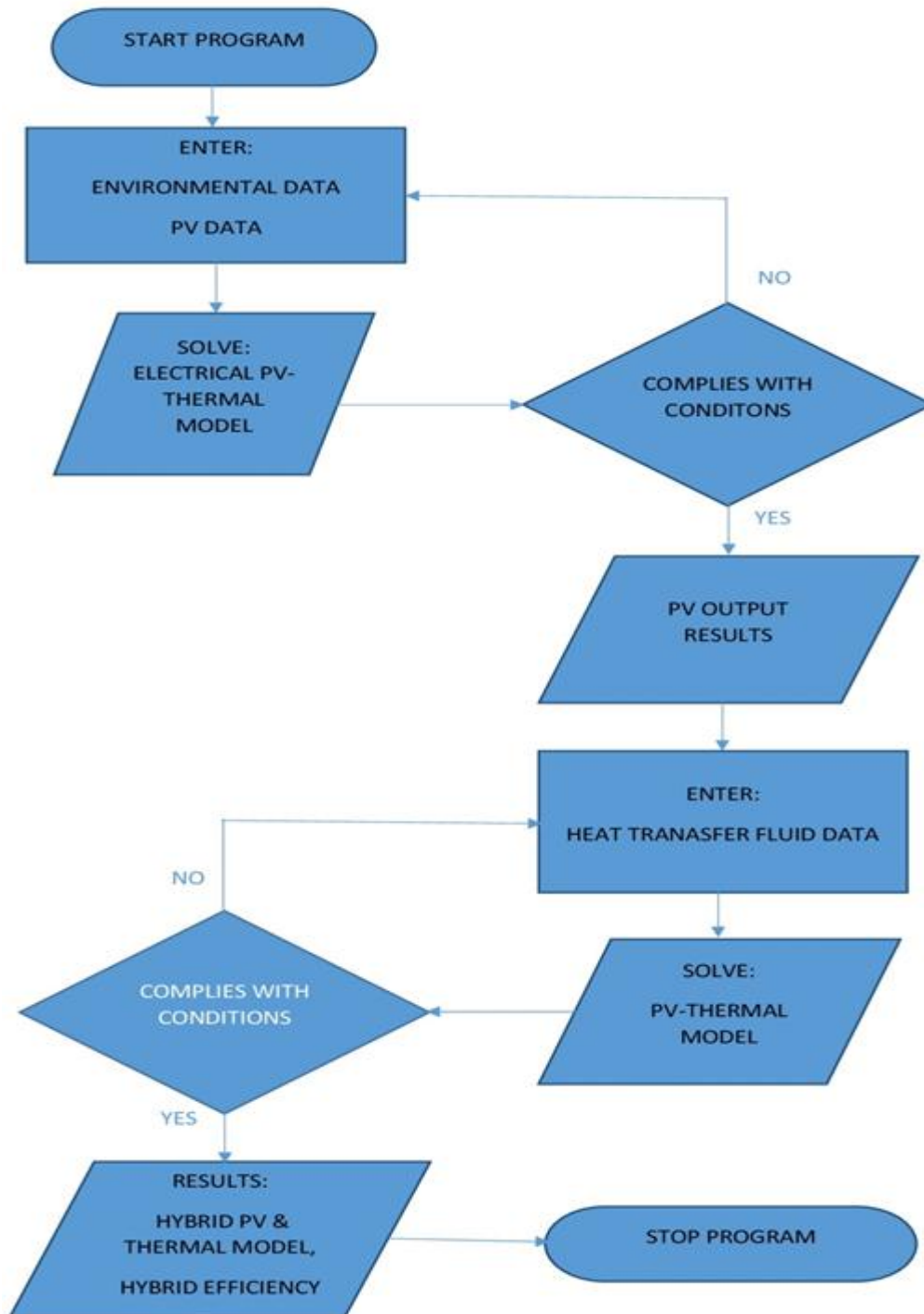


Figure-3. Logical flow chart



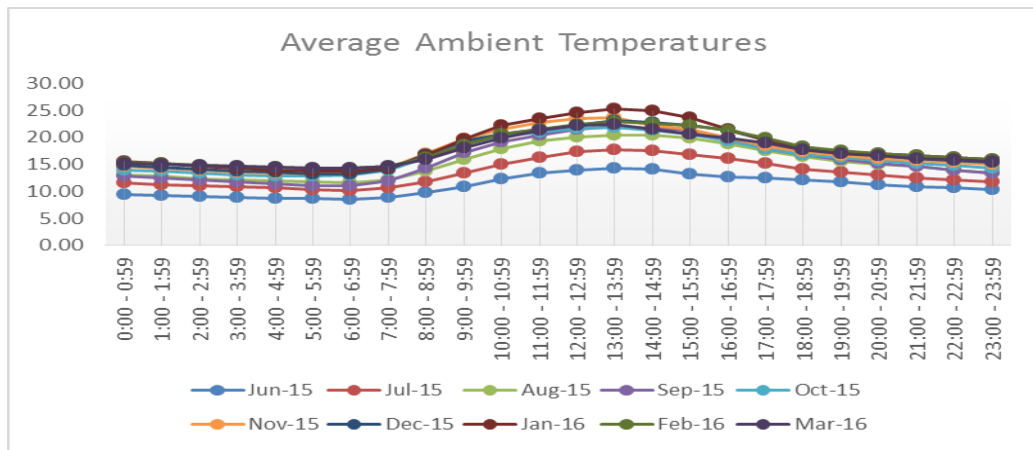


Figure-4. Ambient temperatures (°C) profile 2015-2016

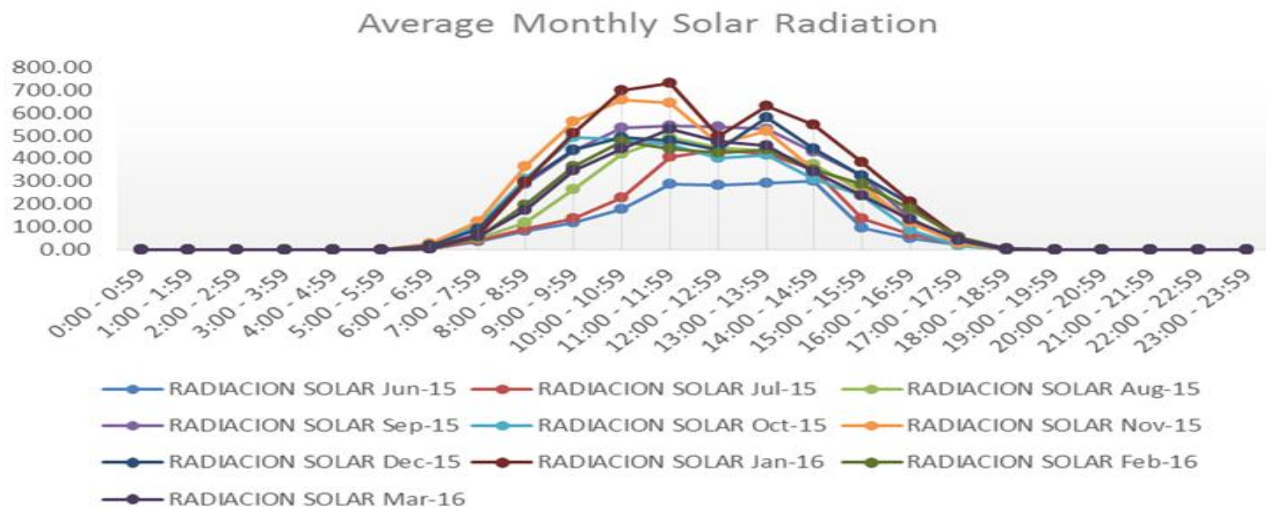


Figure-5. Solar irradiances (w/m²) Profile 2015-2016

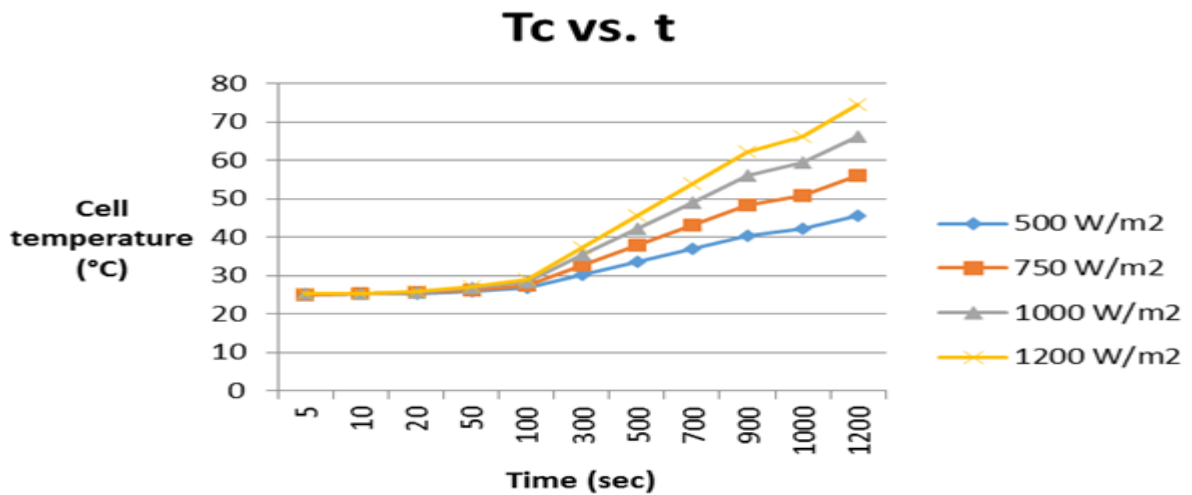


Figure-6. Cell temperature at heat exchanger temperature difference 15 C

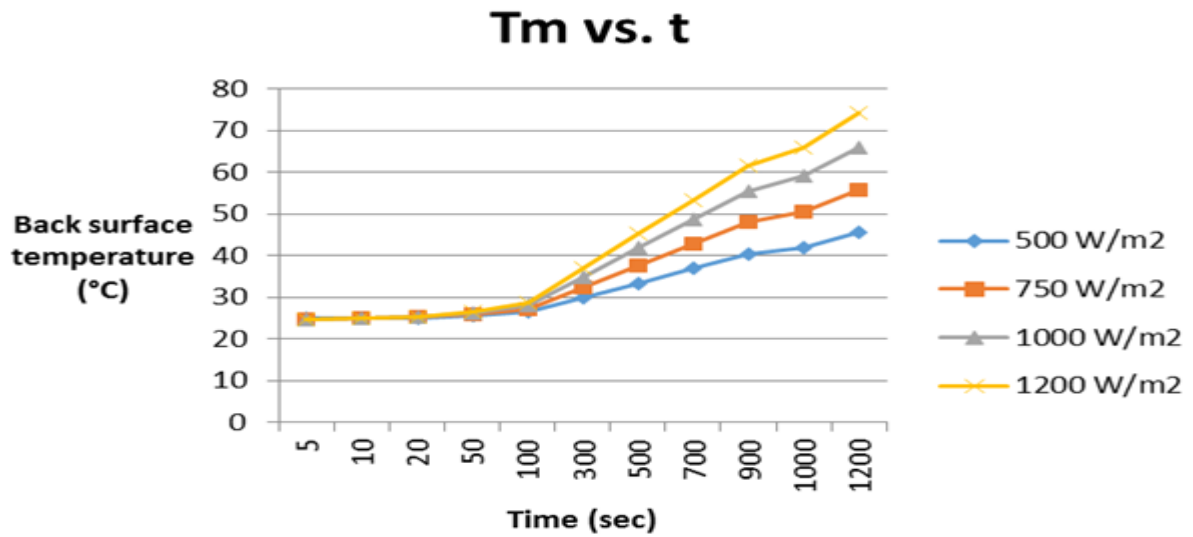


Figure-7. Back PV Cell temperature at heat exchanger temperature difference 15 °C.

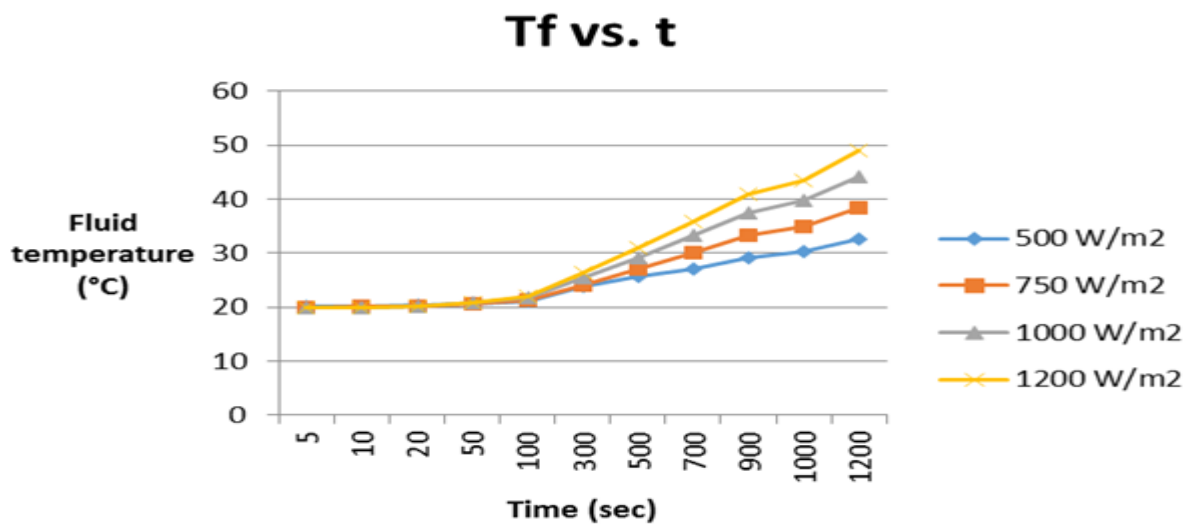


Figure-8. Fluid temperature at heat exchanger temperature difference 15 °C.

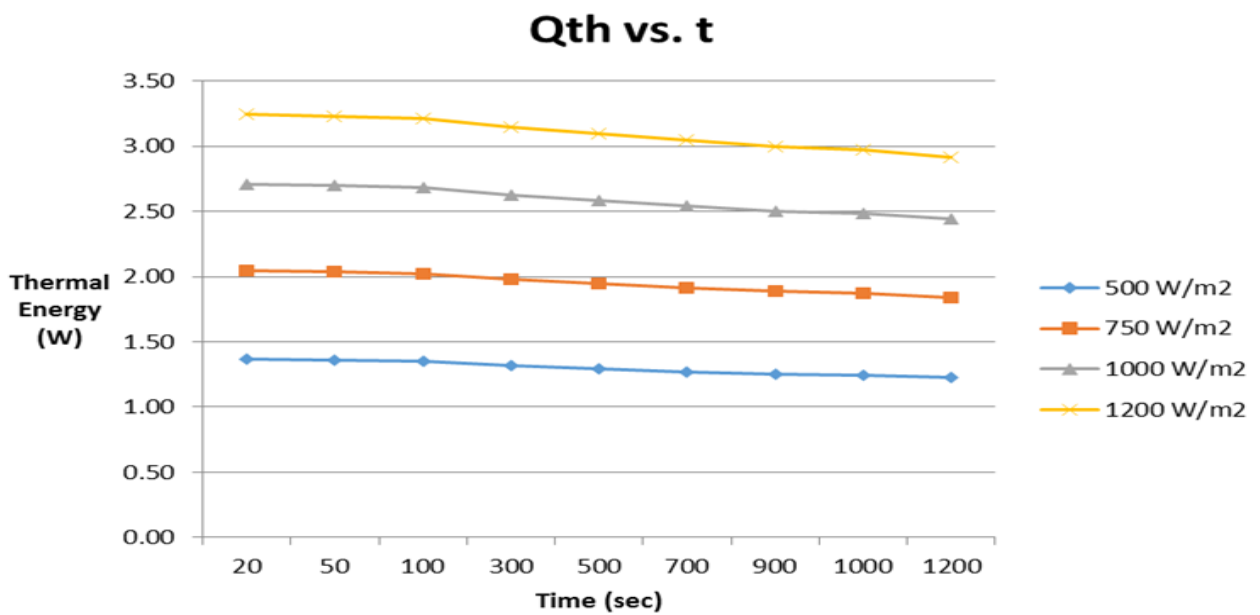


Figure-9. Heat absorbed at different solar radiations and heat exchanger temperature difference 15 °C.



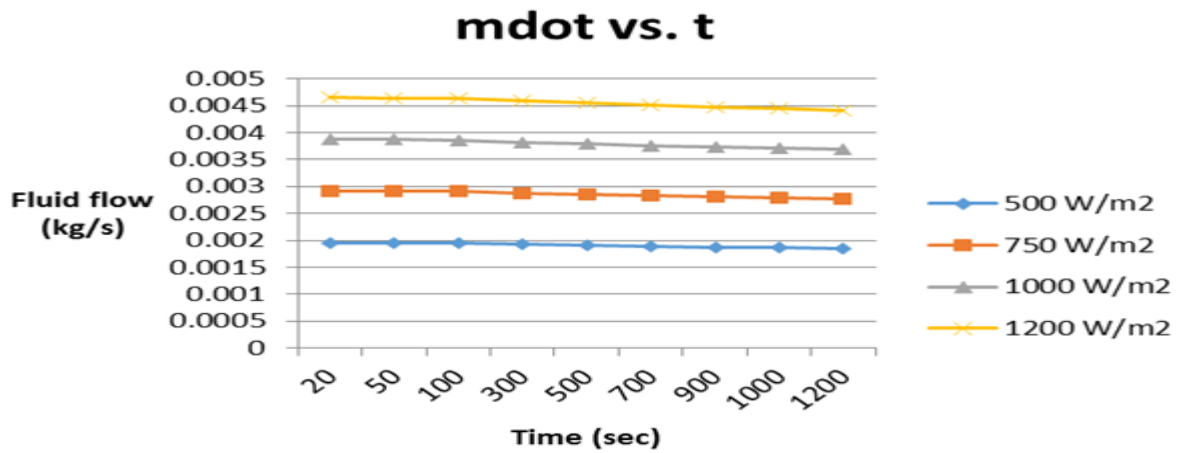


Figure-10. Water mass flow rate at different solar radiations and heat exchanger temperature difference 15 °C.

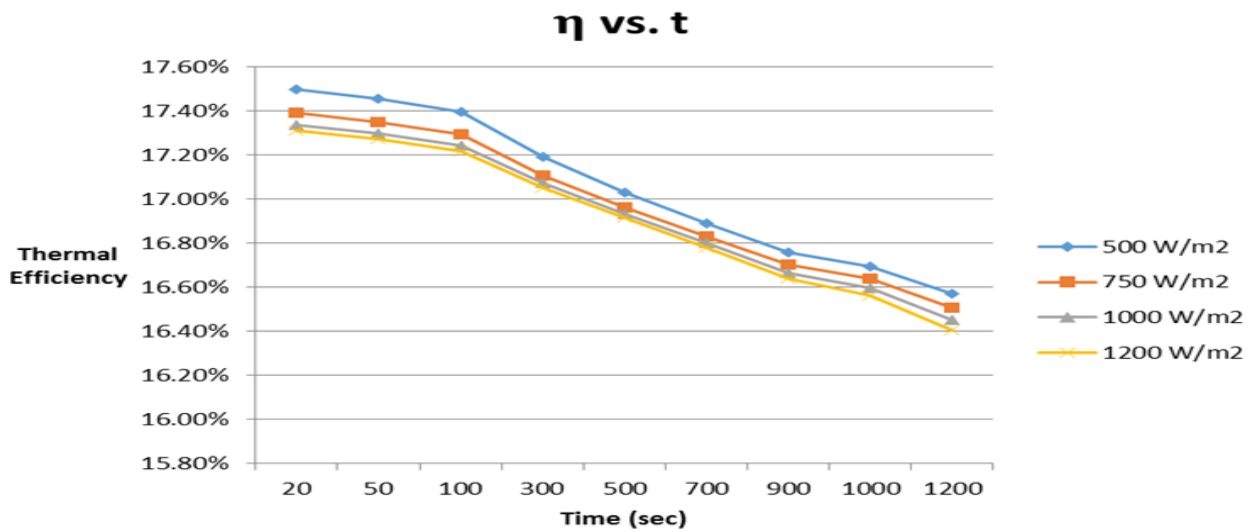


Figure-11. Thermal system efficiency at different solar radiations and heat exchanger temperature difference 15 °C.

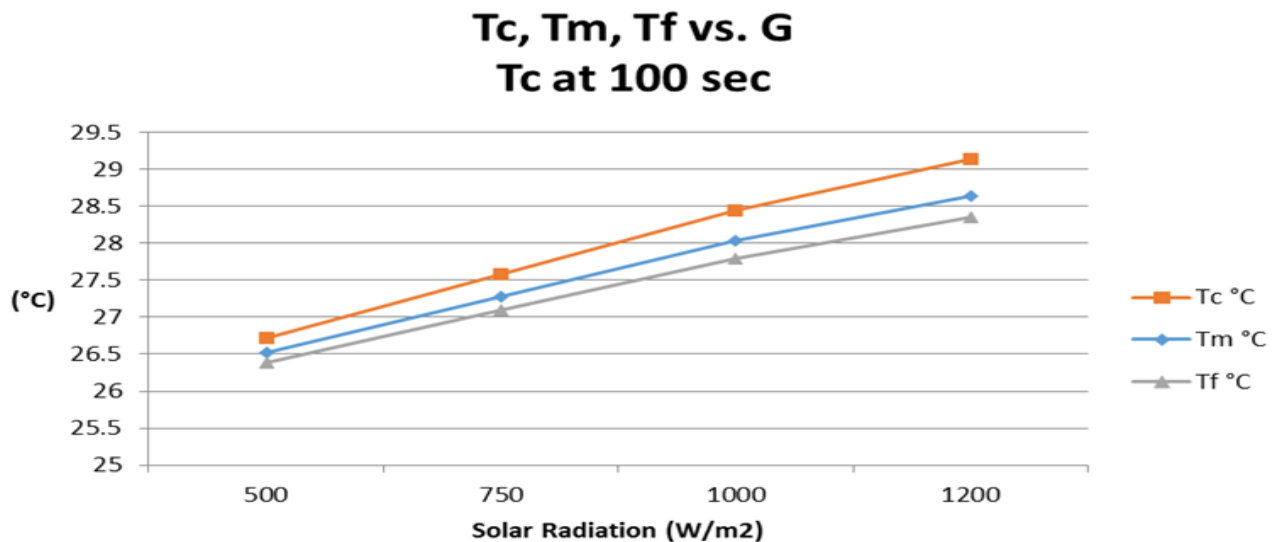


Figure-12. Hybrid system temperatures at different solar radiations and heat exchanger temperature difference 15 °C.

### $\eta$ Hybrid System vs. G Tc at 300 sec

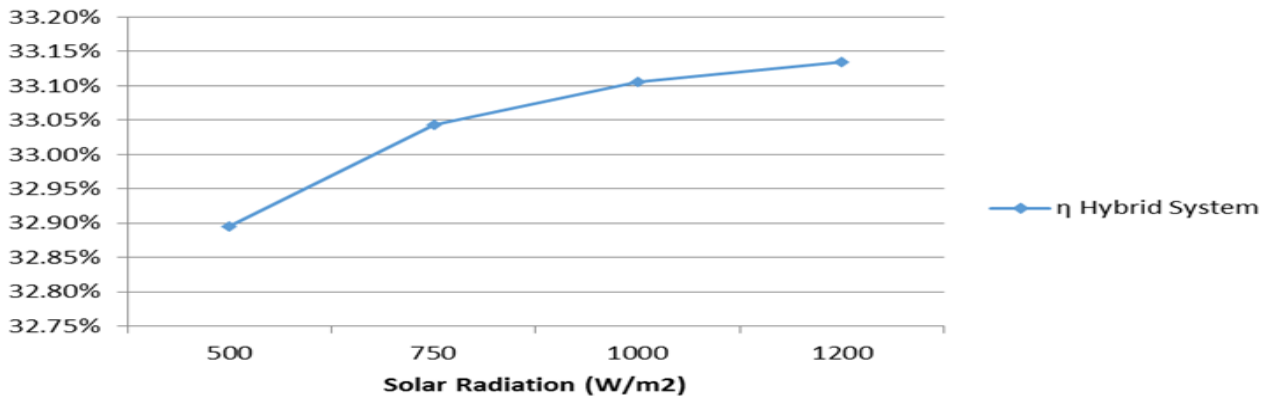


Figure-13. Hybrid system efficiency at different solar radiations and heat exchanger temperature difference 15 °C.

### $\eta$ vs. G Tc at 300 sec

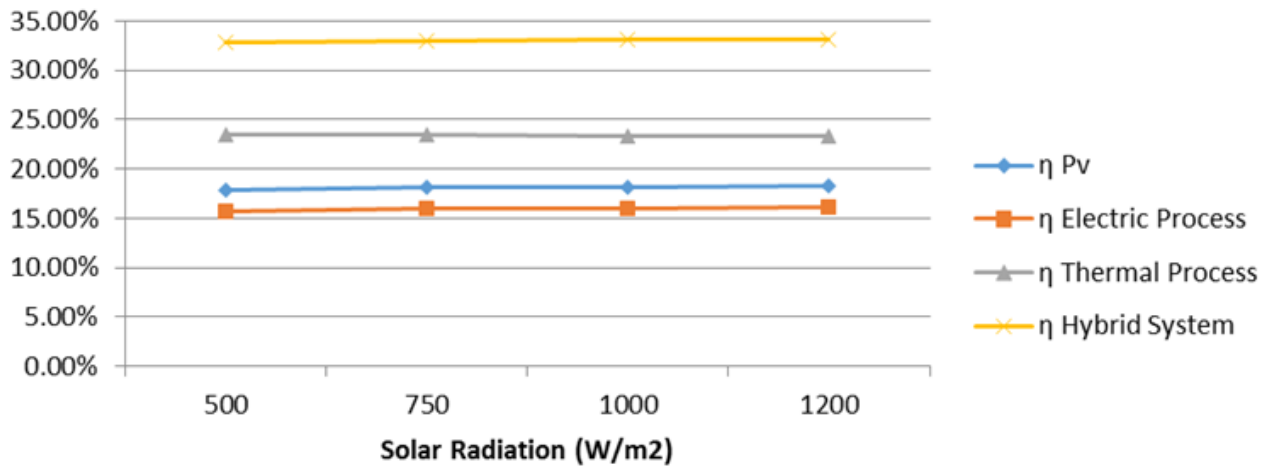


Figure-14. Hybrid system efficiencies at different solar radiations and heat exchanger temperature difference 15 °C.

### Tc-Tf vs. $\eta$ Hybrid System

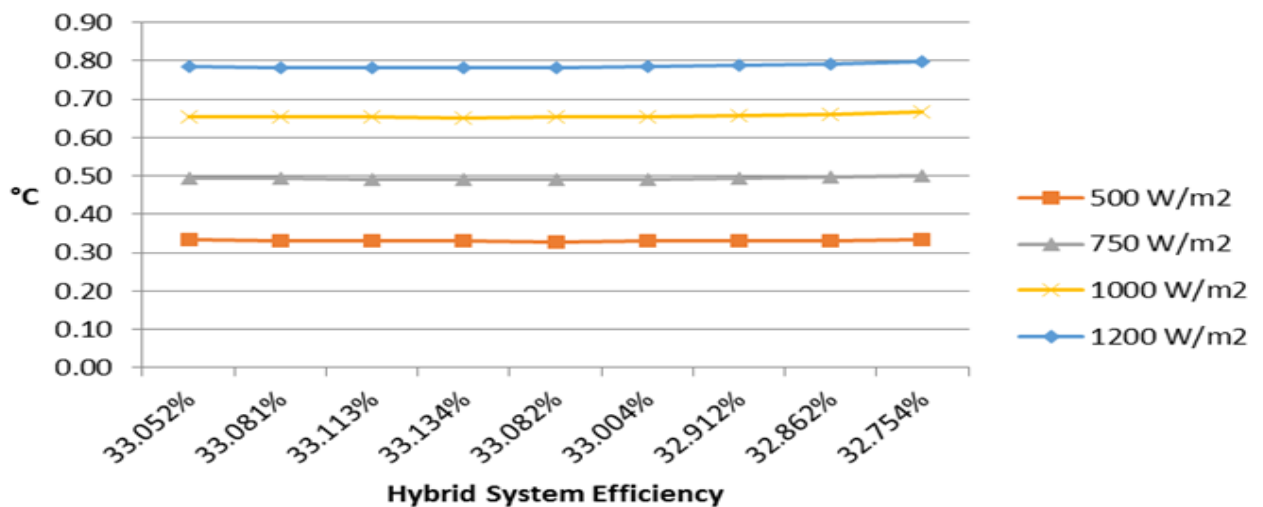


Figure-15. Hybrid system efficiencies at different solar radiations

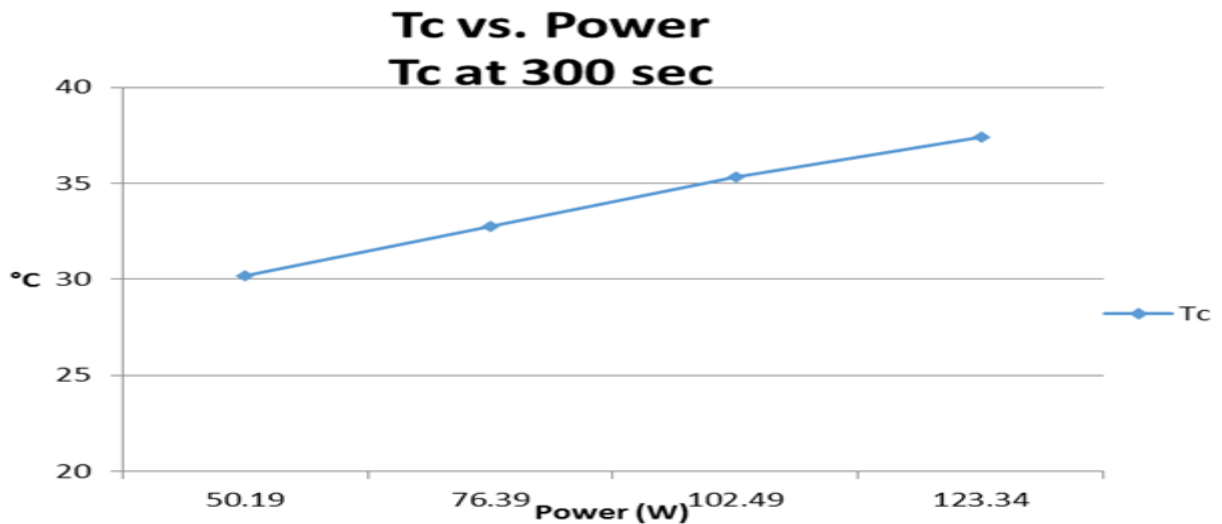


Figure-16. PV power at different PV cell temperature.

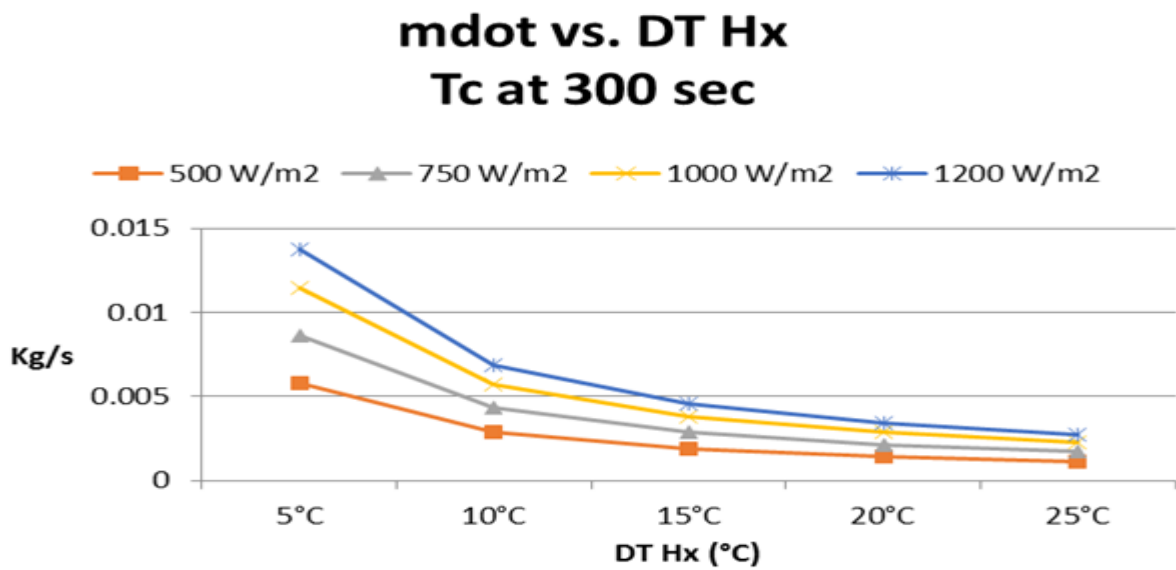


Figure-17. Thermal tubes flow rate at different temperature difference.

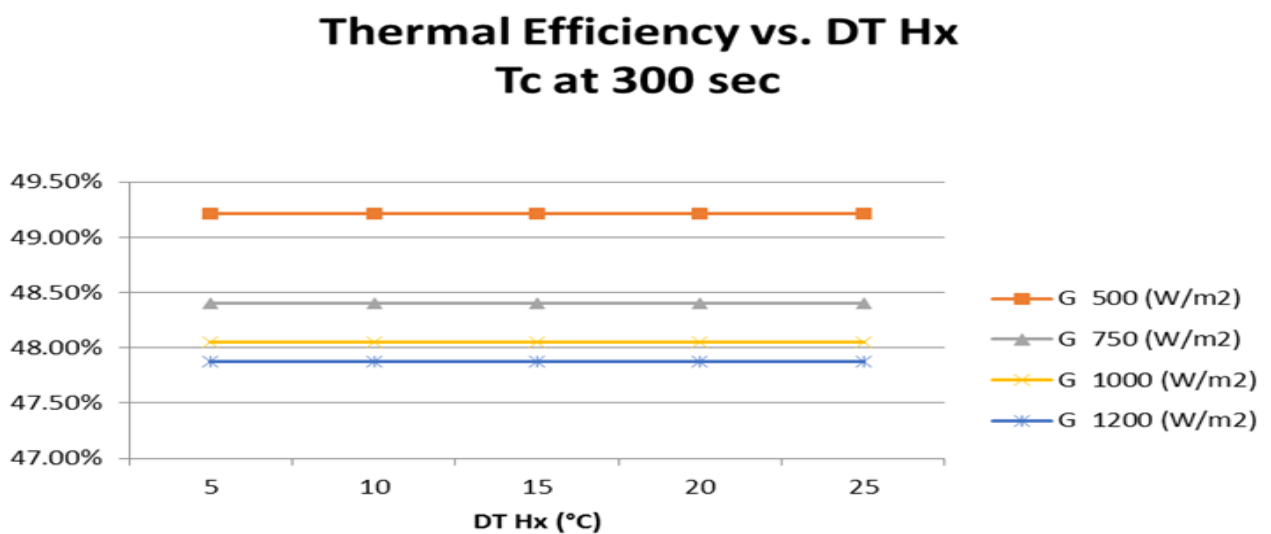


Figure-18. Thermal efficiency at different solar radiations.

## $\eta$ Hybrid System vs. DT HX Tc at 300 sec

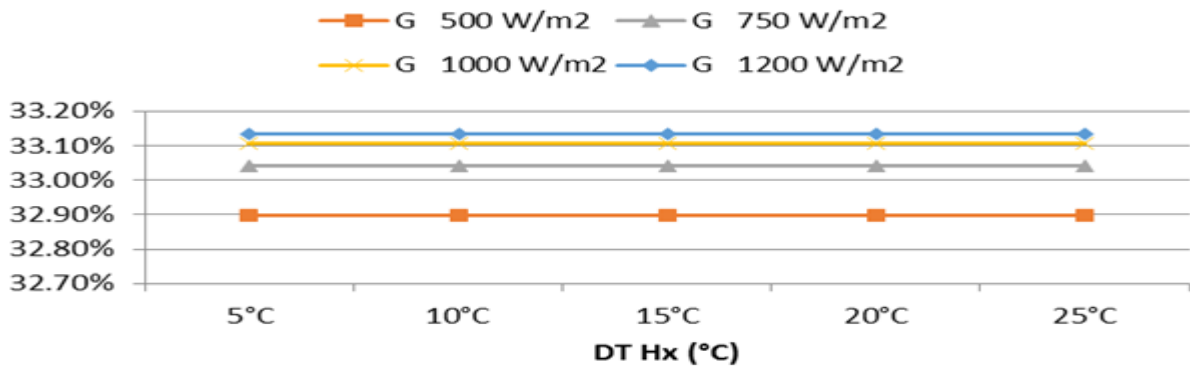


Figure-19. Hybrid efficiency at different solar radiations.

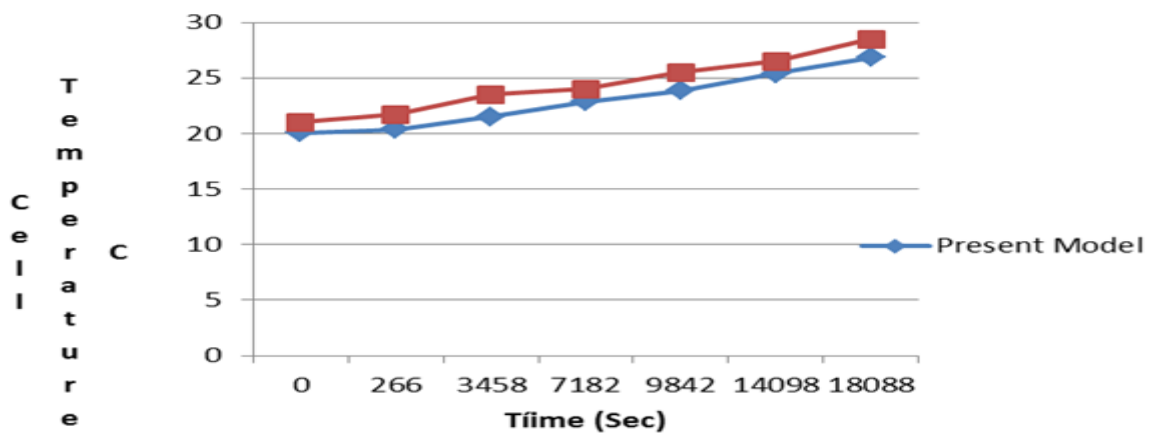


Figure-20. Comparison between present model prediction for cell temperature and Fargali *et al.* (2010) data [16].

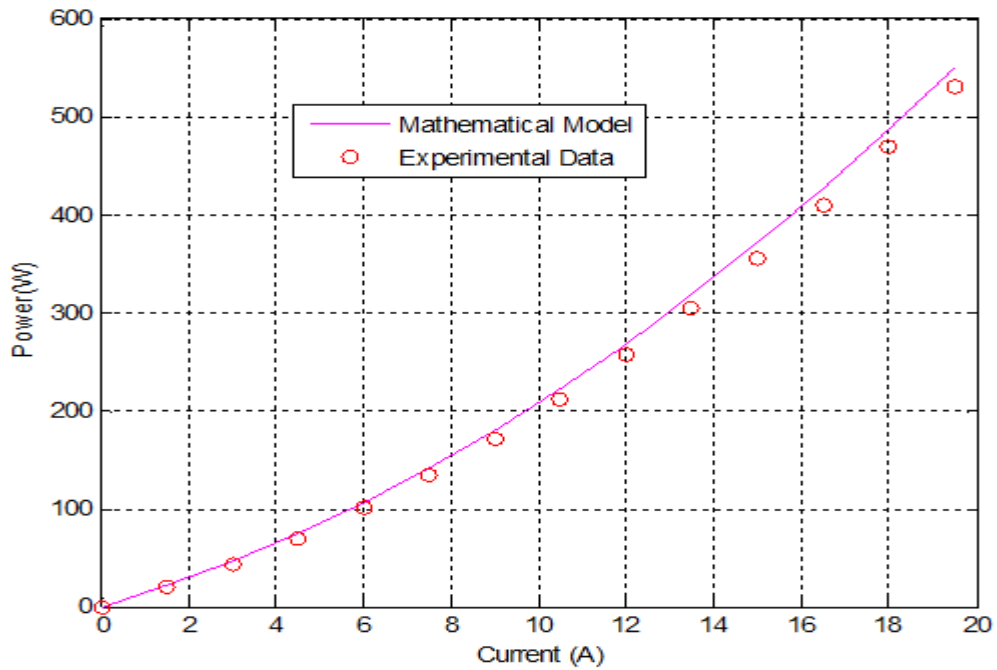


Figure-21. Comparison between present model predictions of PV characteristics [15, 16].

Source: This paper and Sami and Marin (2017). And Fargali *et al.* (2010)

## Nomenclature

Area <sub>cell</sub>	PV cell area (m <sup>2</sup> )
Area <sub>pipe</sub>	Pipe area (m <sup>2</sup> )
Area <sub>HT</sub>	Heat transfer area (m <sup>2</sup> )
C <sub>p,water</sub>	Thermal capacity of water (J/kgK)
D	Internal Pipe diameter (m)
E <sub>gO</sub>	Bandgap energy of semiconductor (1.1 eV)
G	Total Solar radiation incident on the Pv module (W/m <sup>2</sup> )
H	Convective heat transfer coefficient module (W/m <sup>2</sup> K)
h <sub>water</sub>	Heat transfer coefficient (W/m <sup>2</sup> K)
I	Output current of the Pv module (A)
I <sub>o</sub>	Diode saturation current per module (A)
I <sub>ph</sub>	Light generated current per module or photocurrent (A)
I <sub>rs</sub>	Module reverse saturation current (A)
I <sub>sc</sub>	Short circuit current (A)
k	Boltzmann's constant (1.3806503*10 <sup>-23</sup> J/K)
K <sub>i</sub>	Short-circuit of a Pv cell at SRC (mA/°C)
K <sub>Pv</sub>	Thermal conductivity of Pv cell (W/mK)
L <sub>cell</sub>	Length of a Pv cell (m)
$\dot{m}$	Water flow (Kg/s)
mC <sub>p,module</sub>	Thermal capacity of the Pv module (9250 J/K)
m <sub>water</sub>	Mass of water (Kg)
n	Ideality factor of the diode (q)
N <sub>p</sub>	Total number of cells connected in parallel
N <sub>pipes</sub>	Number of pipes
N <sub>s</sub>	Total number of cells connected in series
nTE	Number of Thermal Elements in a pipe
P	Power generated by Pv module (W)
P <sub>a</sub>	Atmospheric pressure of moist air (Pa)
p <sub>w</sub>	Partial pressure of water vapor in moist air (Pa)
q	Electronic charge (C)
Q <sub>conduction</sub>	Energy due to conduction (W in Electrical Process) (W/m <sup>2</sup> in Thermal Process)
Q <sub>convection</sub>	Energy due to convection (W in Electrical Process) (W/m <sup>2</sup> in Thermal Process)
Q <sub>elect</sub>	Electrical power generated (W)
Q <sub>in</sub>	Energy received due to Solar irradiation (W/m <sup>2</sup> )
Q <sub>in_cell</sub>	Energy incident on one Pv cell due to solar radiation (W/m <sup>2</sup> )
Q <sub>radiation</sub>	Energy due to radiation (W/m <sup>2</sup> in Thermal Process)
Q <sub>Thermal</sub>	Energy from thermal process (W)
R <sub>d</sub>	Fouling factor - or unit thermal resistance of the deposit (m <sup>2</sup> K/W)
R <sub>s</sub>	Diode series resistance per module (Ω)
R <sub>sh</sub>	Diode shunt resistance per module (Ω)
S <sub>c</sub>	Total surface area of Pv cells in a module (m <sup>2</sup> )
S <sub>p</sub>	Total area of the PV module (m <sup>2</sup> )
T	Operating temperature (k)

T	Time (s)
$T_a$	Ambient temperature ( $^{\circ}\text{C}$ )
$T_C$	Pv Cell Temperature ( $^{\circ}\text{C}$ )
$T_{db}$	Dry bulb temperature ( $^{\circ}\text{C}$ )
$T_f$	Fluid temperature ( $^{\circ}\text{C}$ )
$T_f$	Fluid temperature ( $^{\circ}\text{C}$ )
$T_{f\_in}$	Fluid temperature at inlet ( $^{\circ}\text{C}$ )
$T_{fHx}$	Maximum temperature at the Heat Exchanger ( $^{\circ}\text{C}$ )
$T_{fHx+1}$	Fluid temperature at thermal element 1 (dx) ( $^{\circ}\text{C}$ )
$T_m$	Module Back-surface temperature ( $^{\circ}\text{C}$ )
$T_r$	Nominal temperature (298.15 K)
U	Thermal conductance of clean heat exchanger ( $\text{W}/\text{m}^2\text{K}$ )
Ud	Thermal conductance of heat exchanger after fouling ( $\text{W}/\text{m}^2\text{K}$ )
V	Output voltage (V)
$V_{oc}$	Open circuit voltage (V)
Vt	Diode thermal voltage (V)
x	Humidity ratio ( $\text{kg}_{\text{water}}/\text{kg}_{\text{dry\_air}}$ )
$\alpha_{abs}$	Overall absorption coefficient
$\eta_{Hybrid}$	Hybrid system efficiency
$\eta_{Pv}$	PV module efficiency
$\eta_{Thermal}$	Efficiency of thermal process
$\rho_w$	Density of water vapor ( $\text{Kg}/\text{m}^3$ )
$\partial Q$	Convection heat transfer rate
$\varepsilon$	Emissivity PV cell
$\sigma$	Stefan-Boltzmann constant ( $5.67\text{E}-08, \text{W}/\text{m}^2\text{K}^4$ )

**Funding:** The research work presented in this paper was made possible through the support of the Catholic University of Cuenca.

**Competing Interests:** The authors declare that they have no competing interests.

**Contributors/Acknowledgement:** Both authors contributed equally to the conception and design of the study.

## REFERENCES

- Armstrong, S. and W.G. Hurley, 2010. A thermal model for photovoltaic panels under varying atmospheric conditions. Applied Thermal Engineering, 30(11-12): 1488-1495. [View at Google Scholar](#) | [View at Publisher](#)
- Bergene and O.M. Lovvik, 1995. Model calculations on a flat-plate solar heat-collector with integrated solar cells. Solar Energy, 55(6): 453-462. [View at Google Scholar](#) | [View at Publisher](#)
- Bradley, F.J. and G.-M. Ernesto, 2012. Modeling a combined photovoltaic-thermal solar panel. Proceedings of the 2012 COMSOL Conference in Boston.
- Chen, H., B.S. Riffat and Y. Fu, 2011. Experimental study on a hybrid photovoltaic/heat pump system. Applied Thermal Engineering, 31(17-18): 4132-4138. [View at Google Scholar](#) | [View at Publisher](#)
- Duffie, J., 1991. Solar engineering of thermal process. New York: Wiley.
- Fargali, H.M., F.H. Fahmy and M.A. Hassan, 2010. A simulation model for predicting the performance of PV/wind- powered geothermal space heating system in Egypt. Online Journal on Electronics and Electrical Engineering, 2(2): 321-330. [View at Google Scholar](#)

- Gangadevi, R., A. Shobhit and R. Shirsho, 2013. A novel hybrid solar system using nanofluid. International Journal of Engineering Research and Technology, 6(6): 747-752. [View at Google Scholar](#)
- Garge, H.P. and R.K. Agarwal, 1995. Some aspects of a PV/T collector/force circulation flat-plate solar water heater with solar cells. Energy Conversion and Management, 36(2): 87-99. [View at Google Scholar](#) | [View at Publisher](#)
- Huang, B.J. and S.C. Du, 1991. A performance test method for solar thermosyphon-systems. Journal of Solar Energy Engineering 113(3): 172-179. [View at Google Scholar](#) | [View at Publisher](#)
- Lalovi, B., Z. Kiss and H.A. Weakliem, 1986. Hybrid amorphous silicon photovoltaic and thermal solar-collector. Sol Cells, 19(2): 131-138. [View at Google Scholar](#) | [View at Publisher](#)
- Li, J., 2015. Structural optimization of the ORC-based solar thermal power system, Chapter 2, structural optimization and experimental investigation of the organic Rankine cycle for solar thermal power generation. Heidelberg: Springer. pp: 41.
- Li, J., G. Pei, Y. Li and J. Ji, 2010. Novel design and simulation of a hybrid solar electricity system with organic Rankine cycle and PV cells. International Journal of Low-Carbon Technologies, 4(5): 223-230. [View at Google Scholar](#) | [View at Publisher](#)
- Rajapakse, A. and S. Chungpaibulpantana, 1994. Dynamic simulation of a photovoltaic r refrigeration system. RERIC, 16(3): 67-101.
- Sami, S. and E. Marin, 2017. A numerical model for predicting performance of solar photovoltaic, biomass and CHP hybrid system for electricity generation. International Journal of Engineering Sciences & Research Technology, 4(1): 1- 22.
- Sami, S. and E. Marin, 2017. Simulation of solar photovoltaic, biomass gas turbine and district heating hybrid system. International Journal of Sustainable Energy and Environmental Research, 6(1): 9-26. [View at Google Scholar](#) | [View at Publisher](#)
- Sami, S. and J. Rivera, 2017. A predictive numerical model for analyzing performance of solar photovoltaic, geothermal hybrid system for electricity generation and district heating. Science Journal Energy Engineering, 5(1): 13-30. [View at Publisher](#)
- Sandnes, B. and J. Rekstad, 2002. A photovoltaic/thermal (PV/T) collector with a polymer absorber plate, experimental study and analytical model. Sol Energy, 72(1): 63-73. [View at Google Scholar](#) | [View at Publisher](#)
- Teo, H.G., P.S. Lee and M.N.A. Hawlader, 2012. An active cooling system for photovoltaic modules. Applied Energy, 90(1): 309-315. [View at Google Scholar](#) | [View at Publisher](#)
- Tripanagnostopoulos, Y., T. Nousia, M. Souliotis and P. Yianoulis, 2002. Hybrid photovoltaic/thermal solar systems. Sol Energy, 72(3): 217-234. [View at Google Scholar](#) | [View at Publisher](#)
- Yang, D.J., Z.F. Yuan, P.H. Lee and H.M. Yin, 2012. Simulation and experimental validation of heat transfer in a novel hybrid solar panel. International Journal of Heat and Mass Transfer, 55(4): 1076-1082. [View at Google Scholar](#) | [View at Publisher](#)
- Zhan, W.B., G.Q. Xu, Y.K. Quan, X. Luo and T.T. Li, 2014. Design and analysis of a novel hybrid solar/gas dish sterling system (HS/GDSS). Applied Mechanics and Materials, 479-480: 575-579. [View at Google Scholar](#)

## BIBLIOGRAPHY

[http://www.engineeringtoolbox.com/fouling-heat-transfer-d\\_1661.html](http://www.engineeringtoolbox.com/fouling-heat-transfer-d_1661.html).

[http://www.engineeringtoolbox.com/water-vapor-saturation-pressure-air-d\\_689.html](http://www.engineeringtoolbox.com/water-vapor-saturation-pressure-air-d_689.html).

<https://en.wikipedia.org/wiki/Humidity>.

*Views and opinions expressed in this article are the views and opinions of the author(s), International Journal of Sustainable Energy and Environmental Research shall not be responsible or answerable for any loss, damage or liability etc. caused in relation to/arising out of the use of the content.*